

# An Overview on X-Rays Images Processing: Methods, Challenges & Issues, and Future Work

Ghulam Gilanie\*, Syeda Naila Batool, Hina Shafique, Aqsa Khursheed, Nimra Mahmood, Sana Cheema,  
Akkasha Latif, Muhammad Sajid, Muhammad Saeed

Department of Artificial Intelligence, Faculty of Computing, The Islamia University of Bahawalpur, Pakistan.

Email addresses: [ghulam.gilanie@iub.edu.pk](mailto:ghulam.gilanie@iub.edu.pk), [nailashah313@gmail.com](mailto:nailashah313@gmail.com), [hinach1912@gmail.com](mailto:hinach1912@gmail.com),  
[aqsakhursheedbwp@gmail.com](mailto:aqsakhursheedbwp@gmail.com), [nimramahmoodbwp@gmail.com](mailto:nimramahmoodbwp@gmail.com), [sanacheema887@gmail.com](mailto:sanacheema887@gmail.com),  
[akashcheema70@gmail.com](mailto:akashcheema70@gmail.com), [mohammad.sajid@iub.edu.pk](mailto:mohammad.sajid@iub.edu.pk), [msaeed4771@gmail.com](mailto:msaeed4771@gmail.com)

**Abstract:** X-Rays imaging is a widely used medical imaging modality to diagnose several diseases in their initial stages. It also has several key applications in the forensic anthropology department. Delayed and erroneous diagnosis may increase mortality and morbidity rate in medical units. Hence, investigation of accurate, autonomous, and automated procedures of diagnosis is of most importance in clinical environments. Machine vision methods proved themselves more accurate and faster at diagnosis desks. In this article, a comprehensive survey with the aims of highlighting importance and uses of X-Rays in clinical and forensic environments, state-of-the-art methods reporting processing of X-Rays images for automated diagnosis of various health disorders present in different anatomical structures, machine-learning techniques to process X-Rays images, benchmarked & publicly available datasets, challenges & issues, and future work is presented. Automated processing of X-Rays image analysis is of utmost concern to every radiology department to speed up diagnosis, prevent mishaps, and reveal new patterns. Dental X-Rays is the easiest and possible method to be adopted to determine faster and easier determination for age and gender on initial investigations for police, courts and other law enforcing agencies. Left hand wrist, femur bone and skull can be used for age assessment, while the pelvic bone can be used to determine gender only. Teeth bone can be used to determine both age and gender. An estimate of height can be made by measuring one of the long bones (Femur or Humerus). Absence or presence of a nasal spine and width of the face has visual clues for racial differences. Several benchmarked datasets exist publicly, however, for forensic anthropology, no sufficient benchmarked dataset exists, which can serve as backbone for the researcher community.

**Keywords:** X-Rays Images Processing, Artificial intelligence, Deep learning, Computer-aided diagnostics

## Introduction

In daily life, a huge amount of radiological data is generated every day in clinical environments (Gilanie, Bajwa, et al., 2018). As compared to this huge amount of data, the number of experts, i.e., radiologists, chest specialists, pulmonologists, medical practitioners and other qualified staff is less in number to interpret this data manually and accurately in a reasonable time (Gilanie, Attique, Naveed, Ahmed, & Ikram, 2013). Automated and trustworthy diagnostic systems are necessary to handle and decrease the number of emergencies and loss (Gilanie, Bajwa, Waraich, & Anwar, 2021; Gilanie, Bajwa, Waraich, Asghar, et al., 2021; Gilanie, Bajwa, Waraich, & Habib, 2019b; Gilanie, Nasir, Bajwa, & Ullah, 2021; Gilanie, Ullah, Mahmood, Bajwa, & Habib, 2018), especially in under developed countries. In remote areas of the world, such systems not only will be available at doorsteps but also can reduce cost of the diagnosis and morbidity & mortality ratio.




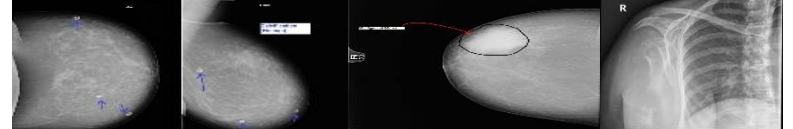
Electromagnetic waves called X-Rays are a type of radiation with short wavelength and high frequency, when passing through body, generate picture in black and white. These rays are used to detect not only fractures in body parts but also to assess soft tissues. This is a common medical test nowadays, suggested by radiologists, orthopedics, and other medical staff in clinical environment. There are different types of X-Rays examination like radiography, fluoroscopy, and computed tomography (CT). Radiography is a process in which a single image is recorded for later evaluation. Fluoroscopy is a live streaming on a monitor for real time monitoring, while CT is a process in which X-Ray images are used as a detector to move around the person. Radiation therapy is a treatment in which X-Rays are used for management of cancer (as a treatment tool). A lead apron must be used while having x-rays test to protect certain parts of the body, because high dose of x-rays while taking images may cause cancer in body or damage tissues specified area. In Pakistan, almost all Govt. hospitals have only analogue (film) X-Rays machines. However, most of the private hospitals have digital X-Rays (DDR) producing both print and DICOM image. Analogue X-Rays film can be converted into digital with the help of a computer and special scanner, available in Pakistan (Asghar, Gilanie, Saddique, & Habib, 2017; Attique et al., 2012; Gilanie, Bajwa, Waraich, & Habib, 2019a).

X-Rays imaging has several key applications in forensic anthropology department to decide accidental and non-accidental bone fracture, age, gender, height, and race estimation and skeletal trauma analysis from bones. It has several applications medical diagnosis including arthritis, chronic obstructive pulmonary disease (COPD), asthma, infections like influenza, lung cancer, fibrosis, dental-decay, consolidation, pleural effusion, pneumothorax, hydro-pneumothorax, miliary shadows/mottling, pneumonia, heart failure, emphysema, tuberculosis, cancer, Covid-19, dislocated joints, abdominal pain, in some instances, fractures and infections, osteoporosis, bone or breast cancer, blocked blood vessels, enlarged of heart, cannon balls, lung-tumor, ILD or interstitial lung disease, etc. detection. X-Rays imaging is also being used in surgery robots, while heart, lungs, chest, prostate, bones, teethes, breasts, joints etc. are the anatomies mostly scanned through it in medical environments. Chest X-Rays (CXR) play a vital role in radiology and pulmonology department, as only CXR may have clues of almost 60% of other physical diseases. CXR may have scans of the heart, lungs, blood vessels, airways, and bones of spine & chest.

Identification has proved to be the most important feature for human beings either living or dead. All proceedings of forensics anthropology department, law enforcement agencies, courts, and other official departments are dependent on human identity facts. These identity facts include face, hair, fingerprint, skin color, eye retina or personal belongings for living persons or dead bodies. Identification becomes most difficult when dead bodies have lost fingerprints and other physical features due to decomposition of human body either fully (only bones) or partially. This can happen due to natural disasters like earthquakes, tsunami, blasts, burning and criminal cases. In October 2005, an earthquake magnitude of 7.6 and had a maximum Mercalli intensity of VIII (Severe) and there were 75000 casualties (Wikipedia, 2005). Many dead bodies lost their identity and /buried temporarily. The officials adopted the methods of matching belongings of dead bodies with information provided by claimants. No autopsy, X-Ray, finger prints and deoxyribonucleic acid (DNA) were performed for the purpose of identification (Morgan, Tidball-Binz, & Van Alphen, 2006). Another crucial incident happened 25th June 2017, at Ahmedpur, Pakistan, when an oil tanker turned turtle, resultantly, 50000-liter petrol spread alongside road. A mob of nearest villagers gathered to collect the petrol but suddenly, the petrol got fired and explosion occurred in a few moments 219 people burned and many of them injured in this tragic incident (Wikipedia, 2017). All dead bodies lost their identity. Over 120 dead victims, who were beyond recognition, were buried in a mass grave. Government of Pakistan announced the amount of Rs.2 million each parent/guardian of dead persons. To claim this amount, more than 10000 people from different families appeared as claimants. Here again the problem was the identification because only bones were left. From 2001 to 2010, in blasts and suicide attacks the total 63898, from them 22657 were civilians, 7127 security personals, 34114 terrorist/insurgents and lost their life (Ali, Yaseen, & Khan, 2020) in Pakistan. Terrorists/insurgents and the victims also lost their identities. In criminal cases, many killers buried the dead bodies of murdered and relaxed that body will be decomposed and it will have lost its identification. It mostly happens in rape case of child and women.

Police department is reported firstly when a fully or partially decomposed dead body is found. They refer the founded materials to the doctor for assessment of the age with the help of intramembranous, endochondral, and wrist test with an assessment difference of two years. This is only used for identification of age greater than 18 and above (Ghimire et al., 2020). When doctor reports, they start further investigation and present the opinion in court or other law enforcement agencies. The doctor is still unable to identify a gender. When no claimant is found in such cases, the police department hands over the bones to the municipal corporation department. The insurgents got relief indirectly. The forensic department always catering such issues on daily basis when they got all data from crime scene. Investigation commences in three dimensions, i.e., identification of murdered, cause of death, and identification of accused. The forensic department uses pathological methods as well as radiological methods in the investigation. There are many methods that can be exercised by the forensic department, which includes finger prints, ossification of bones through X-Ray or CT and DNA (Ghimire et al., 2020). Each of these methods has some limitations regarding its accuracy and availability. DNA is always proved the best one among these. However, if 10,000 people were the claimant of a body, it would not be possible to perform DNA of each of the claimant in a reasonable time. Will each claimant pay for the DNA fee? Because there is only one lab performing available for DNA test in Punjab for the huge volume of population of over 150 million. This problem can be solved if the age and gender of a body is identified initially.

Human bones help us to determine age, gender, height, race, and skeletal trauma analysis. Left hand wrist, femur bone (KC, 2019; Santosh & Pradeep, 2020) and skull (Adserias-Garriga & Wilson-Taylor, 2019; Clarke et al., 2021; Kotěrová et al., 2018; Ubelaker & Khosrowshahi, 2019) can be used for age assessment, while pelvic bone can be used to determine gender only (Y. Li et al., 2019). Further to this, teeth bone can be used to determine both age and gender. Teeth are least affected by external and physical factors than other bones and can be found for long in dead body (Sehrawat & Singh, 2020). Even teeth can survive 1300 years and there are many methods to process medical image of pulp tooth, area ratio, panoramic dental X-Rays. An estimate of height can be made by measuring one of the long bones (Femur or Humerus). Absence or presence of a nasal spine and width of the face has visual clues for racial differences. For skeletal trauma analysis, distinct patterns exist, which are possibly damaged by gunshot wounds and knife wounds, etc. Automated forensic analysis may assist the forensic anthropology department directly, while police, courts, law, and orders and enforcing agencies indirectly. Most common diseases mostly diagnosed through X-Rays scans are enlisted in Figure 1.

| Disease Name  | Images   |
|---------------|--|
| Arthritis     |  |
| Bone Cancer   |  |
| Broken Bones  |  |
| Breast Cancer |  |

|              |  |
|--------------|--|
| Pneumonia    |  |
| Covid-19     |  |
| Dental Decay |  |
| Emphysema    |  |
| Lung Cancer  |  |
| Osteoporosis |  |
| Pneumothorax |  |
| Tuberculosis |  |

Figure 1: Diseases diagnosed through X-Ray scans.

### Challenges and issues

It is radiologically established when only skeleton remain, the identification of gender is more complex and time consuming to determine, hence, pelvic girdle is considered more reliable for gender estimation among all other bones. Moreover, exact estimation of gender is the most difficult task, and it requires some specialist to perform this task. Limited infrastructure and resources are another main issue. No standard benchmarked dataset is available for research to estimate age, gender, height, skeletal trauma analysis, etc. There is a lack of annotations, and activation maps of dataset. Labelled datasets of high quality for training are not yet accessible on a high scale. X-Ray images do not provide 3D information. Bones can block significant diagnostic data as they absorb the radiation. Ligament and muscles do not show up well on X-Ray scans.

Table 1: State-of-the-art methods for computer aided diagnosis using X-Ray images.

| Study  | Reported method  | Dataset detail   | Evaluation measures   | Classification of |
|--|--|--|---|-------------------|
| (Bhandary et al., 2020)                                | Modified AlexNet (MAN)<br>Support vector machine (SVM)     | Total CXR images=2000<br>Pneumonia=1000<br>Normal=1000<br>CT Images (Lung cancer)<br>LIDC-IDRI<br>Total= 500<br>Malignant= 000<br>Benign=500 | CXR Lung cancer<br>Accuracy=96.80%<br>Sensitivity=96.97%<br>Specificity=96.6%<br>CT Lung cancer<br>Accuracy= 97.27%<br>Sensitivity=98.09%<br>Specificity=95.63% | Pneumonia         |
| (Chouhan et al., 2020)                                 | GoogleNet, Alexnet, InceptionV3, DenseNet121, and resnet18 | Total 5232 X-Ray images<br>Normal=1346,<br>Pneumonia=3883.<br>Bacterial<br>Pneumonia=2538,<br>VirusPneumonia=1345                            | AUC= 99.34%<br>Accuracy=96.39%<br>Precision=93.28%  | Pneumonia         |
| (Labhane, Pansare, Maheshwari, Tiwari, & Shukla, 2020) | VGG16, VGG19, and InceptionV3                              | X-Ray images<br>Pneumonia=4273 and<br>Normal=4245  | Accuracy=98 %<br>Precision=0.99%  | Pneumonia         |
| (Park et al., 2019)                                    | Convolutional neural network (CNN)+YOLO model              | X-Ray images<br>pneumothorax=1596<br>and normal=11,137   | AUC=0.984<br>Accuracy=93%<br>Sensitivity= 89.7%<br>Specificity= 96.4%   | Pneumothorax      |
| (Kitamura & Deible, 2020)                              | Support vector machine (SVM)                               | Pneumothorax=5237<br>non-<br>pneumothorax=53066  | AUC=0.90  | Pneumothorax      |
| (Hwang et al., 2020)                                   | Deep learning  | Total 1757 patients<br>Male=1055<br>female=702   | AUC=0.937<br>Sensitivity=70.5%,<br>Specificity=97.7%  | Pneumothorax      |
| (LINDA, 2020)  | COVID-NET  | X-Ray Images<br>Covid-19=68<br>Normal=1203<br>Bacterial Pneumonia<br>Images=931<br>viral Pneumonia=660                                       | Accuracy=92.4%  | COVID-19          |
| (Narin, Kaya, & Pamuk, 2020)                           | ResNet50, InceptionV3, and Inception-ResNetV2              | Total 100 X-ray images<br>Covid-19=50<br>Normal=50   | ResNet50<br>Accuracy= 98%<br>Specificity=100%<br>InceptionV3<br>Accuracy=97%<br>Specificity=100%<br>Inception-ResNetV2<br>Accuracy=87%                          | COVID-19          |

An Overview on X-Rays Images Processing: Methods, Challenges& Issues, and Future Work

|   |   |   |  |              |
|---|---|---|--|--------------|
|   |   |   | Specificity=90%  |              |
| (Ozturk et al., 2020)   | Darknet-19<br>DarkCovidNet                                      | no-findings CXR=500<br>pneumonia CXR=500  | Accuracy=98.08 %   | COVID-19     |
| (Li, Shen, & Luo, 2017)                                       | Stationary wavelets transform (SWT),<br>Multi-scale CIF,<br>SVM | Dataset-1<br>Lung nodules=154<br>Normal=93<br>Dataset-2<br>Abnormal=15<br>Normal=70                   | Sensitivity =78%<br>Sensitivity=90%  | Lung Nodule  |
| (Ausawalaithong, Thirach, Marukatat, & Wilaiprasitporn, 2018) | CNN<br>DenseNet-121   | CXR images=247<br>Lung nodules=154<br>Normal=93   | Accuracy=74.43±6.01 %<br>Sensitivity=74:68±15:33%<br>Specificity=74:96±9:85%   | Lung Cancer  |
| (Li et al., 2020)   | CNN   | Japanese Society of Radiological Technology (JSRT)<br>CXR images=247<br>Lung nodules=154<br>Normal=93 | Area under the Free-Response Receiver Operating Characteristic curve (FAUC)=0.9823   | Lung Nodule  |
| (Gordienko et al., 2018)                                      | UNet(CNN-based)   | CXR images=247<br>Lung nodules=154<br>without lung nodules=93   | Not mentioned  | Lung Cancer  |
| (Liu et al., 2017)  | CNN   | CXR images<br>Total=4701<br>Normal=453<br>TB infected=4248  | Accuracy=85.68 %   | Tuberculosis |
| (Chandra, Verma, Singh, Jain, & Netam, 2020)                  | SVM   | CXR images=800<br>Montgomery=138<br>Shenzhen CXR=662<br>Abnormal images=394<br>Normal images=406      | For Montgomery Dataset<br>Accuracy=95.60 ± 5.07%<br>AUC=0.95 ± 0.06<br>For Shenzhen Dataset<br>Accuracy=99.40 ± 1.05%<br>AUC=0.99 ± 0.01 | Tuberculosis |

|  |   |   |   |                          |
|--|---|---|---|--------------------------|
| (Rahman et al., 2020)  | CNN, ChexNet, DenseNet201   | X-Ray Images<br>TB infected=3500<br>Normal CXR=3500   | Without Segmentation<br>ChexNet<br>Accuracy=96.47%<br>Sensitivity=96.47%<br>Specificity=96.51%<br>With Segmentation<br>DenseNet20<br>Accuracy=98.6%<br>Sensitivity=98.56%<br>Specificity=98.54% | Tuberculosis             |
| (Sahlol, Abd Elaziz, Tariq Jamal, Damaševičius, & Farouk Hassan, 2020) | MobileNet+Artificial Ecosystem-based Optimization (AEO) algorithm | Shenzhen dataset<br>CXR=662<br>Benign=326<br>TB cases=336<br>Dataset 2<br>CXR=5232<br>Pneumonia=3883<br>Normal=2538 | Shenzhen dataset<br>Accuracy=90.2%<br>For Dataset 2<br>Accuracy=94.1%   | Tuberculosis             |
| (Tuan et al., 2018)  | Dental Diagnosis System (DDS) APC+ Algorithm                      | Dental images=87  | Accuracy=92.74%   | Dental Diagnosis         |
| (Bouchahma, Hammouda, Kouki, Alshemali, & Samara, 2019)                | CNN   | Dental X-Ray image=235  | Accuracy=87%.   | Dental decay             |
| (Yang, Cheng, Shimaponda-Nawa, & Zhu, 2019)                            | PCA+ANN   | Fractured=8,035<br>Non-fractured=8,480  | AUC= 0.8271<br>Accuracy=72.89%  | Long-Bone Fracture       |
| (Hrzić, Štajduhar, Tschauer, Sorantin, & Lerga, 2019)                  | Hybrid method Based on local entropy                              | CXR=860<br>Fracture-free images=642<br>Fracture images=218  | Accuracy=91.16%   | Bone Fracture Detection  |
| (Singh, Dutta, Jennane, & Lespessailles, 2017)                         | SVM, k-nearest neighbors, Naïve Bayes, ANN                        | Bones X-Ray images=174<br>Normal=87<br>Osteoporotic fractures=87  | SVM<br>Accuracy=97.87%<br>Sensitivity=100 %<br>Specificity=95.74 %<br>AUC=0.98  | Osteoporosis             |
| (Snehalatha, Rajalakshmi, Gopikrishnan, & Gupta, 2017)                 | GLCM  | RAPatients=30   | RA (N=30)<br>Mean=0.034±0.060%<br>SD=0.147±0.091%   | Rheumatoid Arthritis(RA) |
| (Bandyopadhyay, Biswas, & Bhattacharya, 2019)                          | SVM+ Decision tree  | TCIA dataset<br>Long-bone X-ray images=150<br>Healthy Persons=50<br>Cancer-affected                                 | Accuracy=0.85<br>Sensitivity=0.88<br>Specificity=0.82   | Bone-Cancer              |

|   |   |   |  |  |
|---|---|---|--|--|
|   |   | patients=100  |  |  |
| (Campo, Pascau, & Estépar, 2018)                                | CNN   | X-ray Simulations=7,377   | Sensitivity=85.68%<br>Specificity=80.42%<br>AUC=90.73%   | Emphysema  |
| (Varzandeh et al., 2019)  | Cross section and descriptive analysis. Picture analysis and communication system               | 90 males and 90 females   | Accuracy=77% for ilium height for gender estimation<br>Accuracy=70%for acetabular diameter and breadth                                   | Gender Estimation  |
| (Ilić, Vodanović, & Subašić, 2019)                              | DCN   | 4000 Panoramic Dental X-RAYS (Male 40% and female 60%)                          | Average accuracy=94.3%   | Gender Estimation  |
| (Khdairi, Halilah, Khandakji, Jost-Brinkmann, & Bartzela, 2019) | Demirjian's methodand method of polynomial percentile   | 1260 Orthopantomograms (OPGs) images ofstudents (566 male and 694 female)       | Accuracy=99%   | Finding Difference b/w DA(dental age) CA(Chorological age) |
| (Kumagai et al., 2019)  | Third molar maturity index  | 276 radio gram images of students (139 female 137 males between 14 to 24 years) | Sensitivity (Boys 89% and girls=84%)<br>Specificity (Boys 96% and girls=93%)<br>PPV (Positive Predictive Value) (Boys=92% and girls=87%) | Estimation of Age groups                                   |
| (Avuçlu & Başçiftçi, 2020)                                      | Area, Perimeter, Centre of gravity, Similarity ratio, Radius calculation on dental X-Ray images | 1315 panoramic dental X-Ray images  | -  | Identification of age and gender                           |

**Literature Review**

In this research (Bhandary et al., 2020), modified AlexNet to classify chest X-Ray images has been used. Two datasets, i.e., Chest X-Ray (normal and pneumonia) and Lung CT image (malignant and benign) have been used for research and experiments. Out of total 2000 images of chest X-Ray, 1000 each belong to normal and pneumonia cases, for dataset 1,while out of total 1500 CT images, 1000 are malignant and 500 are benign for dataset 2.Haralick approach is used to extract texture features. Their modelachieved 96% accuracy on X-Ray images. In the article(Shanthi & Rajkumar, 2020), the authors proposed method for lung cancer prediction using



grey level co-occurrence matrix (GLCM) and Gabor filter. They used Stochastic Diffusion Search (SDS) algorithm for feature selection. Neural network, Naive Bayes, and Decision Trees have been used for classification. They used 140 normal and 130 abnormal images obtained from the cancer genome atlas (TCGA) dataset.

In this study (Varzandeh et al., 2019), Picture Analysis and Communication System (PACS) is used to measure height of ilium, inter-acetabular distance, acetabular diameter and pelvic breadth. Dataset of 90 male and 90 female volunteers is used, who were suffering from some skeleton disease or pelvic trauma. The results were varying in accuracy with respect to sensitivity, age group, and genders. The accuracy ranges from 77% for ilium height for gender estimation and 70% for acetabular diameter and breadth. This study is with low accuracy and limited dataset is used for experiments. Another study (Ilić et al., 2019), presented fast and accurate approach for gender estimation from panoramic dental X-Ray images. The classification method is performed on cranial bone images using DCN layered approach. Softmax activation function is used to obtain probabilities in type and frequency of layers. The system is trained to classify images based on their morphological features. 4000 high quality images having dimensions of 3256x1536 with 8-bits per pixel are used as dataset. The dataset contains dental X-Rays of people belonging to different age group and genders (male 40% and female 60%). The results are obtained in four staged experiments with accuracy as >82%. On other hand, the result accuracy is above 90% in age grouping (between 20 to 80 years), but accuracy decreases dramatically and shows 50% when age is above 80 years. Average accuracy of this study is 94.3%, which is good. This study can be used to estimate the age as well as race of a person. A study reported by (Khdairi et al., 2019), used dataset of 1260 students among them 566 male and 694 female for age estimation. They used Demirjian's method, center of linear regression, and polynomial percentile and achieved accuracy equal to 99% DA (dental age) and CA (Chronological age) estimation. By measuring length and width of third molar index used with statistical approach, the age is estimated in a study reported by (Kumagai et al., 2019). Dataset of 276 students (139 females and 137 males) with age between 14 to 24 years, is used. Results are based on sensitivity (boys=89% and girls=84%), specificity (boys=96% and girls=93%). This study has an issue of very small dataset. Another research reported by (Ayuçlu & Başçiftçi, 2020) focused on identification of age and gender from panoramic dental X-Ray to facilitate forensics. The methods used center of gravity, area, perimeter, similarity, and ratio of teeth after applying basic image processing. 1315 panoramic dental X-Ray images are used as dataset and all teeth images got specified labels, which include gender, age, tooth number and count. The average results are 89%.

The article (Chouhan et al., 2020) proposed a transfer learning based approach for pneumonia detection from chest X-ray images. A total of 5232 images were used for experiments with an overall and combined accuracy as 96.39%. In this research paper (X. Li et al., 2019) CNN model has been used for pneumothorax detection from chest CT scans of 280 patients. A support vector machine (SVM) has been used for classification with overall accuracy as 96.5%, sensitivity as 100% and specificity as 82.5%. In a study (Hwang et al., 2020), a deep learning algorithm has been used for the inspection of pneumothorax from chest radiographs. The dataset includes 1757 patient images with achieved ROC, sensitivity, and specificity as 0.937, 70.5%, and 97.7%, respectively for the identification of pneumothorax. In the paper reported by (Chan, Zeng, Wu, Wu, & Sun, 2018), the chest X-Ray images are used for lung-related diseases identification. SVM is used to train on uniform local binary pattern (ULBP) features to classify normal and abnormal lungs. Dataset used for this research includes 32 chest radiographs, including traumatic pneumothorax and spontaneous pneumothorax. The 5-fold cross-validation result shows 82.2% accuracy. In this article (Kitamura & Deible, 2020), pneumothorax detecting method has been proposed. The open-source chest X-ray (CXR8) dataset, in which 4696 pneumothorax (PTX) and 41946 non-PTX images have been used for training and testing. The model attained area under the curve as 0.90. In the research (Park et al., 2019), convolutional neural network (CNN) is used to detect the pneumothorax from chest x-ray. CNN has been trained using "You Only Look Once" (YOLO) model. To evaluate and validate the CNN model for the detection of pneumothorax, dataset of 253 pneumothorax patients and 250 normal was used. The sensitivity, specificity, and AUC of pneumothorax detection was 89.7%, 96.4%, and 0.984 respectively. In this study (Taylor, Mielke, & Mongan, 2018), a convolutional neural network model is used to detect the pneumothorax from chest x-ray images. The dataset contains 13,292 frontal chest X-rays including 3,107 with pneumothorax. Dataset is split into 70%, 15%, 15% for training, validation, and testing respectively. Maximum

values achieved against sensitivity, specificity, and AUC are 0.84, of 0.97, and of 0.96 respectively. Recently reported state-of-the-art methods for computer aided diagnosis-using X-Ray images are presented in Table 1.

**Datasets of X-Ray Images**

There are some publicly available datasets as shown in Table 2. These datasets contain X-Ray images of different diseases. A comprehensive detail these datasets is as follows.

**Pneumonia**

This dataset has normal pneumonia cases. Normal case images are 1583, while pneumonia case images are 4273. This dataset is publicly available published by Kaggle.

**NIH Chest X-rays**

The National institute of Health ChestX-Ray dataset is a large dataset with 30,000 patient’s data. This dataset has 112,000 chest X-Ray images of 14 diseases. Kaggle also published this dataset.

**COVID-19**

Covid-19 is an infectious disease; with the passage of time, it becomes a serious pandemic. It has three types of cases, i.e., Covid-19, normal, and pneumonia with 576, 1583, and 4273 images respectively. Kaggle also published this.

**Fracture Bones**

Fractured bones images of X-Ray images are publicly available on Medpix. It has more than 100 types of fractured images with total 3242 number of images.

**Table 2: Benchmarked and publicly available datasets**

| Dataset          | Publisher | Diseases  | Number of Cases                            | Link  |
|------------------|-----------|---|--|---|
| Pneumonia        | Kaggle    | Pneumonia   | Normal=1583<br>Pneumonia=4273              | <a href="https://www.kaggle.com/paultimothymooney/chest-xray-pneumonia">https://www.kaggle.com/paultimothymooney/chest-xray-pneumonia</a>   |
| NIH chest X-Rays | Kaggle    | Atelectasis, Cardiomegaly, Effusion, Infiltration Mass, Nodule, Pneumonia, Pneumothorax, Consolidation, Edema, Emphysema, Fibrosis, Pleural, Thickening, and Hernia | Total X-Rays images=112,120                | <a href="https://www.kaggle.com/nih-chest-xrays/data">https://www.kaggle.com/nih-chest-xrays/data</a>   |
| Covid-19         | Kaggle    | Covid pneumonia   | Covid=576<br>Normal=1583<br>Pneumonia=4273 | <a href="https://www.kaggle.com/prashant268/chest-xray-covid19-pneumonia/">https://www.kaggle.com/prashant268/chest-xray-covid19-pneumonia/</a>   |
| Fracture bones   | Medpix    | Navicular fracture, Sacral, Insufficiency, Distal fabular, Pisiform, Scapular, T12, Colle’s, Smith, Moore’s   | Total X-Rays images=3242                   | <a href="https://medpix.nlm.nih.gov/search?allen=true&amp;allt=true&amp;allit=true&amp;query=fracture">https://medpix.nlm.nih.gov/search?allen=true&amp;allt=true&amp;allit=true&amp;query=fracture</a> |

**Machine-learning methods to process X-Rays images**

On the platform of machine learning, several methods are used to process X-Rays images for auto decision making. A few of these methods assisting computer-aided diagnostics are shown in Figure 2. As per the literature reviewed, Deep Learning (Deep Convolutional Networks), Convolutional Neural Networks (CNN), and Support Vector Machines (SVMs) proved themselves to be helpful for X-Rays image processing. Deep Learning (DL) techniques are the most widely and successful techniques and became promising predictive technology with near human-level accuracy. CNN among DL techniques is a popular one, winning various image processing-based challenges. Various CNN architectures including GoogleNet, Alexnet, InceptionV3, DenseNet121, Resnet18 etc.

have shown their applicability in the literature. Although CNN is a layered architecture, it also requires following some important hyper-parameters.

**Learning Rate:** Learning rate is the most important hyper parameter. It is a hyper-parameter that controls how much the model changes each time the model weights are changed in response to the expected error. It is represented by  $\eta$ . It defines how quickly a network updates its parameters. A low learning rate slows down the learning process but converges smoothly. A larger learning rate speeds up the learning but may not converge. Usually, a decaying learning rate is preferred. The optimal learning ranges from 0.1 to exponentially lower values: 0.01, 0.001, etc.

**Momentum:** Momentum is the direction of the next step with the knowledge of the previous steps. A typical choice of momentum is between 0.5 to 0.9.

**Number of epochs:** An epoch is one learning cycle where the model sees the whole training dataset. It specifies how many times the learning algorithm can go through the entire training dataset. It can vary according to the available datasets.

**Batch size:** Mini batch size is the number of sub samples given to the network after which parameter update happens. A good default value for batch size could be 32. It can vary from 32, 64, 128, 256, and so on.

SVM on the other hand also remained successful in terms of memory efficiency for the classification of several disorders embodied through X-Ray scanners. It uses hyper-plane for classification process to separate features of data classes. It selects a location away from the features of the classes to determine a line. The distances of each class are measured according to the hyper-plane determined by the SVM method. It has come up with linear and non-linear versions. Like CNN, it also has tuning of several its apartness including choice of appropriate kernel and its parameters, choosing between hard margin /soft margin, etc. literature also revealed that in some cases, while dealing with X-Rays images, features are extracted using CNN models, and SVM is used for the classification on these extracted features (Toğaçar, Ergen, & Cömert, 2020).

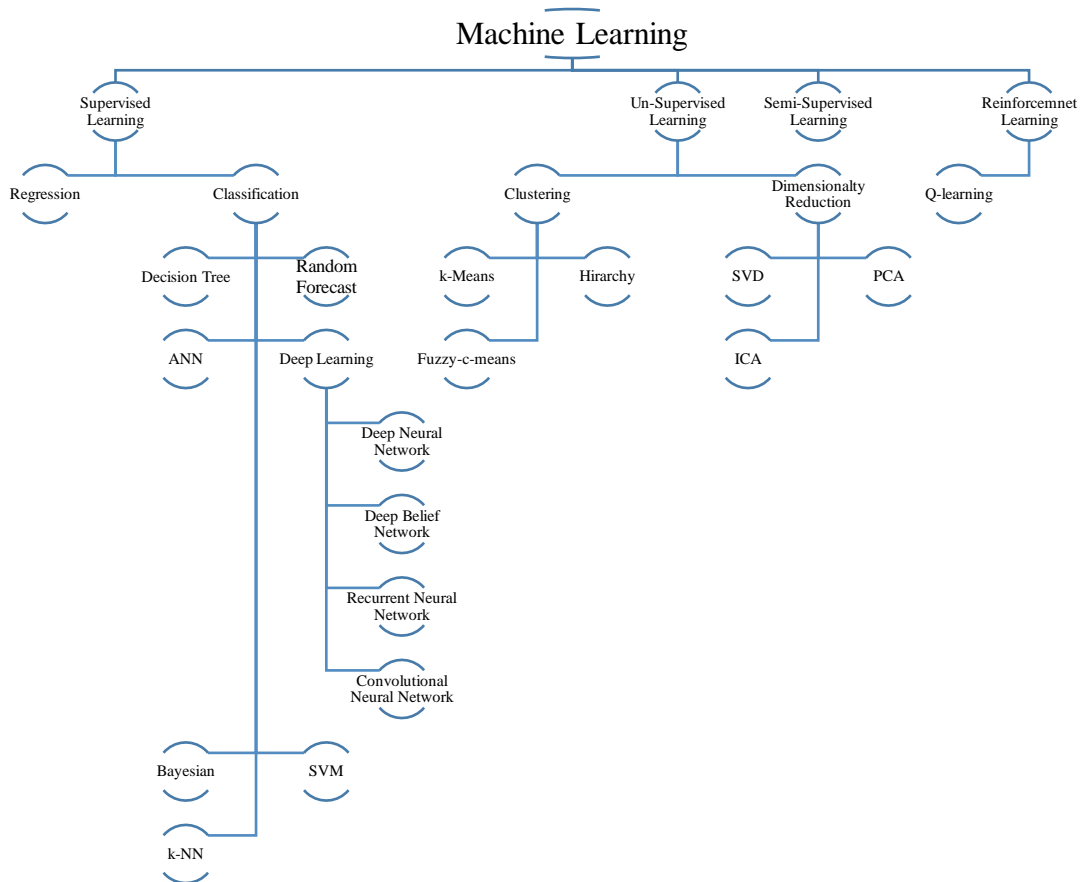


Figure 2: Machine-learning models assisting computer aided diagnostics.

## Conclusion

It is established from the literature review that X-Ray imaging is widely used medical imaging modality to diagnose health disorders. Automated processing of X-Ray image analysis is of utmost concern to every radiology department to speed up diagnosis, prevent mishaps, and reveal new patterns. X-Ray imaging also has several key applications in forensic anthropology department. Machine vision methods proved themselves more accurate, cost effective, and faster at diagnosis, forensic, analysis, evaluation, etc. Dental X-Ray is the easiest method to be adopted to determine age and gender on initial investigations by police, courts and other law enforcing agencies. Left hand wrist, femur bone and skull can be used for age assessment, while the pelvic bone can be used to determine gender only. Teeth bone can be used to determine both age and gender. Teeth are less affected by external and physical factors than other bones, hence, can be found after a long time in dead body. An estimate of height can be made by measuring one of the long bones (femur or humerus). Absence or presence of a nasal spine and width of the face has visual clues for racial differences. For skeletal trauma analysis, distinct patterns exist, which are possibly damaged by gunshot wounds and knife wounds, etc. Several benchmarked datasets exist publicly, however, for forensic anthropology, no sufficient datasets exist, which can serve as backbone for the researcher community.

## References

- Adserias-Garriga, J., & Wilson-Taylor, R. (2019). Skeletal age estimation in adults *Age Estimation* (pp. 55-73): Elsevier.
- Ali, Q., Yaseen, M. R., & Khan, M. T. I. (2020). The impact of temperature, rainfall, and health worker density index on road traffic fatalities in Pakistan. *Environmental Science and Pollution Research*, 1-20.
- Asghar, K., Gilanie, G., Saddique, M., & Habib, Z. (2017). Automatic enhancement of digital images using cubic Bézier curve and Fourier transformation. *Malaysian Journal of Computer Science*, 30(4), 300-310.
- Attique, M., Gilanie, G., Mehmood, M. S., Naweed, M. S., Ikram, M., Kamran, J. A., & Vitkin, A. (2012). Colorization and automated segmentation of human T2 MR brain images for characterization of soft tissues. *PLoS one*, 7(3), e33616.
- Ausawalaithong, W., Thirach, A., Marukat, S., & Wilaiprasitporn, T. (2018). *Automatic lung cancer prediction from chest X-ray images using the deep learning approach*. Paper presented at the 2018 11th Biomedical Engineering International Conference (BMEICON).
- Avuçlu, E., & Başçiftçi, F. (2020). The determination of age and gender by implementing new image processing methods and measurements to dental X-ray images. *Measurement*, 149, 106985.
- Bandyopadhyay, O., Biswas, A., & Bhattacharya, B. B. (2019). Bone-cancer assessment and destruction pattern analysis in long-bone X-ray image. *Journal of digital imaging*, 32(2), 300-313.
- Bhandary, A., Prabhu, G. A., Rajinikanth, V., Thanaraj, K. P., Satapathy, S. C., Robbins, D. E., . . . Raja, N. S. M. (2020). Deep-learning framework to detect lung abnormality—A study with chest X-Ray and lung CT scan images. *Pattern Recognition Letters*, 129, 271-278.
- Bouchahma, M., Hammouda, S. B., Kouki, S., Alshemali, M., & Samara, K. (2019). *An automatic dental decay treatment prediction using a deep convolutional neural network on X-Ray images*. Paper presented at the 2019 IEEE/ACS 16th International Conference on Computer Systems and Applications (AICCSA).
- Campo, M. I., Pascau, J., & Estépar, R. S. J. (2018). *Emphysema quantification on simulated X-rays through deep learning techniques*. Paper presented at the 2018 IEEE 15th International Symposium on Biomedical Imaging (ISBI 2018).
- Chan, Y.-H., Zeng, Y.-Z., Wu, H.-C., Wu, M.-C., & Sun, H.-M. (2018). Effective pneumothorax detection for chest X-ray images using local binary pattern and support vector machine. *Journal of healthcare engineering*, 2018.
- Chandra, T. B., Verma, K., Singh, B. K., Jain, D., & Netam, S. S. (2020). Automatic detection of tuberculosis related abnormalities in Chest X-ray images using hierarchical feature extraction scheme. *Expert Systems with Applications*, 158, 113514.

- Chouhan, V., Singh, S. K., Khamparia, A., Gupta, D., Tiwari, P., Moreira, C., . . . De Albuquerque, V. H. C. (2020). A novel transfer learning based approach for pneumonia detection in chest X-ray images. *Applied Sciences*, 10(2), 559.
- Clarke, J., Peyre, H., Alison, M., Bargiacchi, A., Stordeur, C., Boizeau, P., . . . Léger, J. (2021). Abnormal bone mineral density and content in girls with early-onset anorexia nervosa. *Journal of Eating Disorders*, 9(1), 1-8.
- Ghimire, S., Miramini, S., Edwards, G., Rotne, R., Xu, J., Ebeling, P., & Zhang, L. (2020). The investigation of bone fracture healing under intramembranous and endochondral ossification. *Bone Reports*, 100740.
- Gilanie, G., Attique, M., Naweed, S., Ahmed, E., & Ikram, M. (2013). Object extraction from T2 weighted brain MR image using histogram based gradient calculation. *Pattern Recognition Letters*, 34(12), 1356-1363.
- Gilanie, G., Bajwa, U. I., Waraich, M. M., & Anwar, M. W. (2021). Risk-free WHO grading of astrocytoma using convolutional neural networks from MRI images. *Multimedia Tools and Applications*, 80, 4295-4306.
- Gilanie, G., Bajwa, U. I., Waraich, M. M., Asghar, M., Kousar, R., Kashif, A., . . . Rafique, H. (2021). Coronavirus (COVID-19) detection from chest radiology images using convolutional neural networks. *Biomedical Signal Processing and Control*, 66, 102490.
- Gilanie, G., Bajwa, U. I., Waraich, M. M., & Habib, Z. (2019a). Automated and reliable brain radiology with texture analysis of magnetic resonance imaging and cross datasets validation. *International Journal of Imaging Systems and Technology*, 29(4), 531-538.
- Gilanie, G., Bajwa, U. I., Waraich, M. M., & Habib, Z. (2019b). Computer aided diagnosis of brain abnormalities using texture analysis of MRI images. *International Journal of Imaging Systems and Technology*, 29(3), 260-271.
- Gilanie, G., Bajwa, U. I., Waraich, M. M., Habib, Z., Ullah, H., & Nasir, M. (2018). Classification of normal and abnormal brain MRI slices using Gabor texture and support vector machines. *Signal, Image and Video Processing*, 12(3), 479-487.
- Gilanie, G., Nasir, N., Bajwa, U. I., & Ullah, H. (2021). RiceNet: convolutional neural networks-based model to classify Pakistani grown rice seed types. *Multimedia Systems*, 1-9.
- Gilanie, G., Ullah, H., Mahmood, M., Bajwa, U. I., & Habib, Z. (2018). Colored Representation of Brain Gray Scale MRI Images to potentially underscore the variability and sensitivity of images. *Current Medical Imaging*, 14(4), 555-560.
- Gordienko, Y., Gang, P., Hui, J., Zeng, W., Kochura, Y., Alienin, O., . . . Stirenko, S. (2018). *Deep learning with lung segmentation and bone shadow exclusion techniques for chest X-ray analysis of lung cancer*. Paper presented at the International Conference on Computer Science, Engineering and Education Applications.
- Hrzić, F., Štajduhar, I., Tschauer, S., Sorantin, E., & Lerga, J. (2019). Local-entropy based approach for X-ray image segmentation and fracture detection. *Entropy*, 21(4), 338.
- Hwang, E. J., Hong, J. H., Lee, K. H., Im Kim, J., Nam, J. G., Choi, H., . . . Park, C. M. (2020). Deep learning algorithm for surveillance of pneumothorax after lung biopsy: a multicenter diagnostic cohort study. *European radiology*, 1-12.
- Ilić, I., Vodanović, M., & Subašić, M. (2019). *Gender Estimation from Panoramic Dental X-ray Images using Deep Convolutional Networks*. Paper presented at the IEEE EUROCON 2019-18th International Conference on Smart Technologies.
- KC, S. (2019). *Development of Human Age and Gender Identification System from Teeth, Wrist and Femur Images*. Paper presented at the Proceedings of International Conference on Sustainable Computing in Science, Technology and Management (SUSCOM), Amity University Rajasthan, Jaipur-India.
- Khdairi, N., Halilah, T., Khandakji, M. N., Jost-Brinkmann, P.-G., & Bartzela, T. (2019). The adaptation of Demirjian's dental age estimation method on North German children. *Forensic science international*, 303, 109927.
- Kitamura, G., & Deible, C. (2020). Retraining an open-source pneumothorax detecting machine learning algorithm for improved performance to medical images. *Clinical imaging*, 61, 15-19.

- Kotěřová, A., Navega, D., Štepanovský, M., Buk, Z., Brůžek, J., & Cunha, E. (2018). Age estimation of adult human remains from hip bones using advanced methods. *Forensic science international*, 287, 163-175.
- Kumagai, A., Takahashi, N., Palacio, L. A. V., Giampieri, A., Ferrante, L., & Cameriere, R. (2019). Accuracy of the third molar index cut-off value for estimating 18 years of age: validation in a Japanese samples. *Legal Medicine*, 38, 5-9.
- Labhane, G., Pansare, R., Maheshwari, S., Tiwari, R., & Shukla, A. (2020). *Detection of pediatric pneumonia from chest x-ray images using cnn and transfer learning*. Paper presented at the 2020 3rd International Conference on Emerging Technologies in Computer Engineering: Machine Learning and Internet of Things (ICETCE).
- Li, X., Shen, L., & Luo, S. (2017). A solitary feature-based lung nodule detection approach for chest X-ray radiographs. *IEEE journal of biomedical and health informatics*, 22(2), 516-524.
- Li, X., Shen, L., Xie, X., Huang, S., Xie, Z., Hong, X., & Yu, J. (2020). Multi-resolution convolutional networks for chest X-ray radiograph based lung nodule detection. *Artificial intelligence in medicine*, 103, 101744.
- Li, X., Thrall, J. H., Digumarthy, S. R., Kalra, M. K., Pandharipande, P. V., Zhang, B., . . . Li, Q. (2019). Deep learning-enabled system for rapid pneumothorax screening on chest CT. *European journal of radiology*, 120, 108692.
- Li, Y., Huang, Z., Dong, X., Liang, W., Xue, H., Zhang, L., . . . Deng, Z. (2019). Forensic age estimation for pelvic X-ray images using deep learning. *European Radiology*, 29(5), 2322-2329. doi:10.1007/s00330-018-5791-6
- LINDA, W. (2020). A tailored deep convolutional neural network design for detection of covid-19 cases from chest radiography images. *Journal of Network & Computer Applications*, 20, 1-12.
- Liu, C., Cao, Y., Alcantara, M., Liu, B., Brunette, M., Peinado, J., & Curioso, W. (2017). *TX-CNN: Detecting tuberculosis in chest X-ray images using convolutional neural network*. Paper presented at the 2017 IEEE international conference on image processing (ICIP).
- Morgan, O., Tidball-Binz, M., & Van Alphen, D. (2006). *Management of dead bodies after disasters: a field manual for first responders*. Retrieved from
- Narin, A., Kaya, C., & Pamuk, Z. (2020). Automatic detection of coronavirus disease (covid-19) using x-ray images and deep convolutional neural networks. *arXiv preprint arXiv:2003.10849*.
- Ozturk, T., Talo, M., Yildirim, E. A., Baloglu, U. B., Yildirim, O., & Acharya, U. R. (2020). Automated detection of COVID-19 cases using deep neural networks with X-ray images. *Computers in biology and medicine*, 121, 103792.
- Park, S., Lee, S. M., Kim, N., Choe, J., Cho, Y., Do, K.-H., & Seo, J. B. (2019). Application of deep learning-based computer-aided detection system: detecting pneumothorax on chest radiograph after biopsy. *European radiology*, 29(10), 5341-5348.
- Rahman, T., Khandakar, A., Kadir, M. A., Islam, K. R., Islam, K. F., Mazhar, R., . . . Mahub, Z. B. (2020). Reliable tuberculosis detection using chest X-ray with deep learning, segmentation and visualization. *IEEE Access*, 8, 191586-191601.
- Sahlol, A. T., Abd Elaziz, M., Tariq Jamal, A., Damaševičius, R., & Farouk Hassan, O. (2020). A novel method for detection of tuberculosis in chest radiographs using artificial ecosystem-based optimisation of deep neural network features. *Symmetry*, 12(7), 1146.
- Santosh, K., & Pradeep, N. (2020). Knowledge Discovery (Feature Identification) from Teeth, Wrist and Femur Images to Determine Human Age and Gender *Machine Learning with Health Care Perspective* (pp. 133-158): Springer.
- Sehrawat, J. S., & Singh, M. (2020). Application of Trace Elemental Profile of Known Teeth for Sex and Age Estimation of Ajnala Skeletal Remains: a Forensic Anthropological Cross-Validation Study. *Biological Trace Element Research*, 193(2), 295-310. doi:10.1007/s12011-019-01712-8
- Singh, A., Dutta, M. K., Jennane, R., & Lespessailles, E. (2017). Classification of the trabecular bone structure of osteoporotic patients using machine vision. *Computers in biology and medicine*, 91, 148-158.

- Snehalatha, U., Rajalakshmi, T., Gopikrishnan, M., & Gupta, N. (2017). Computer-based automated analysis of X-ray and thermal imaging of knee region in evaluation of rheumatoid arthritis. *Proceedings of the Institution of Mechanical Engineers, Part H: Journal of Engineering in Medicine*, 231(12), 1178-1187.
- Taylor, A. G., Mielke, C., & Mongan, J. (2018). Automated detection of moderate and large pneumothorax on frontal chest X-rays using deep convolutional neural networks: A retrospective study. *PLoS medicine*, 15(11), e1002697.
- Toğaçar, M., Ergen, B., & Cömert, Z. (2020). COVID-19 detection using deep learning models to exploit Social Mimic Optimization and structured chest X-ray images using fuzzy color and stacking approaches. *Computers in biology and medicine*, 121, 103805.
- Tuan, T. M., Fujita, H., Dey, N., Ashour, A. S., Ngoc, V. T. N., & Chu, D.-T. (2018). Dental diagnosis from X-ray images: an expert system based on fuzzy computing. *Biomedical Signal Processing and Control*, 39, 64-73.
- Ubelaker, D. H., & Khosrowshahi, H. (2019). Estimation of age in forensic anthropology: historical perspective and recent methodological advances. *Forensic Sciences Research*, 4(1), 1-9.
- Varzandeh, M., Akhlaghi, M., Farahani, M. V., Mousavi, F., Jashni, S. K., & Yousefinejad, V. (2019). The Diagnostic value of anthropometric characteristics of ilium for sex estimation using pelvic radiographs. *International Journal of Medical Toxicology and Forensic Medicine*, 9(1), 1-10.
- Wikipedia. (2005). 2005 Kashmir earthquake. Retrieved from [https://en.wikipedia.org/wiki/2005\\_Kashmir\\_earthquake](https://en.wikipedia.org/wiki/2005_Kashmir_earthquake)
- Wikipedia. (2017). 2017 Bahawalpur explosion. Retrieved from [https://en.wikipedia.org/wiki/2017\\_Bahawalpur\\_explosion](https://en.wikipedia.org/wiki/2017_Bahawalpur_explosion)
- Yang, A. Y., Cheng, L., Shimaponda-Nawa, M., & Zhu, H.-Y. (2019). *Long-bone fracture detection using Artificial Neural Networks based on line features of X-ray images*. Paper presented at the 2019 IEEE Symposium Series on Computational Intelligence (SSCI).